



# GRID BASED SOLAR POWERED WATER PUMPING WITH MULTILEVEL INVERTER USING BLDC MOTOR DRIVE

Jalla Upendar<sup>1</sup>, Sana Arsheen<sup>2</sup>, Sapavath Sreenu<sup>3</sup>

<sup>1,2 and 3</sup>Department of Electrical Engineering, University College of Engineering, Osmania University, India.

**ABSTRACT:** A solar photovoltaic (PV) water pumping system with bidirectional power flow control is proposed in this research. The brushless DC (BLDC) motor-drive without phase current sensors is used to power the pump. The water pump may be operated at full capacity, around-the-clock, and in any weather, thanks to this device's ability to provide electricity to a single-phase utility grid when not in use for pumping water. You can get the most out of your photovoltaic array and your motor-pump, and you can rest assured that your pumping system will work when you need it to. A single-phase voltage source converter (VSC) using a unit vector template (UVT) generating technique is used to regulate bidirectional power flow between the grid and the DC bus of a voltage source inverter (VSI) that supplies a brushless DC motor (BLDC). The VSI's switching loss is minimized when it operates at its fundamental frequency. This method allows for a PV array to operate at its MPP while also correcting power factor and lowering the total harmonic distortion (THD) of the grid. The flexibility and reliability of the MATLAB/Simulink platform have been demonstrated through a variety of simulation findings that have been implemented in hardware.

**Keywords:** Power flow control, Solar photovoltaic, Brushless DC motor, Voltage source converter, Unit vector template, Maximum power point(MPP), Power quality, Power factor and Total harmonic distortion(THD).

## 1. INTRODUCTION

The Power converters, due to their excellent efficiency, low learning curve, and ease of use, have become indispensable in all industrial control applications[1]-[4]. They contribute greatly to renewable energy systems due to the advantages of low-cost conversion circuits and optimal utilization of renewable power under varied input conditions. Because changing voltage levels call for different combinations of standard Single Input Single Output (SISO) DC-DC converters with different voltage gains, SISO system control is more difficult and costly[5]-[9].

Single Input Multi Output (SIMO) conversion circuits have allowed for significant advancements in the field of power converters. One of the most promising avenues of investigation in this subject is the use of these innovative DC-DC converters to boost and stabilize the low and fluctuating renewable energy output voltage for the DC link of grid/load connected systems based on inverters. It is suggested that SIMO converters be utilized to successfully balance the DC-link voltage of loads. SIMO conversion is appealing to many scientists since it includes Buck Boost (BB) operation[10]. The use of BB logic and the incorporation of shoot through states are also prohibited in conventional siso converters. Different areas of SIMO, such as structural alterations, applications with different sources, and control strategies, have been the focus of research.

Electricity generation relies heavily on the utilization of renewable energy sources. Renewable energy sources such as the sun, the wind, and the earth's geothermal heat are all viable options for generating power. Silicon solar photovoltaic (PV) modules directly convert solar energy into electrical energy, making them a practical option for power generation. Multiple solar PV cells are serially joined to form a module. The module current rating increases when the cell area is increased, and vice versa. By connecting multiple PV modules in series and parallel, a solar PV array is created, which may be used to generate more electricity. Numerous studies are being conducted to enhance the materials and techniques used to harness solar energy, as its uses expand. Solar cell efficiency, intensity of source radiation, and storage methods are the primary determinants of collection efficiency [11]-[13]. The materials used to create solar cells place a cap on the devices' efficiency. Because it is challenging to achieve significant increases in cell performance, the collection procedure as a whole is less efficient[14]. The most practical approach to enhancing solar power's efficiency is to boost the amount of solar energy collected. Maximizing power extraction in solar systems can be done in two main ways. Either they orbit around the sun or they are based on the MPP [15]-[18].

The two power sources are an engine driven alternator and battery bank. That makes up the load-adaptive variable-speed producing system. When the energy from the alternator is not enough to meet unanticipated spikes in load demand, energy is pumped from the battery to the dc link. The battery's energy is replenished when the engine's capacity is overextended [19]-[21].

Battery charger and DC/DC converter combined in an integrated dc UPS topology [22]. When there is a power outage, the battery feeds the load naturally via a diode linked between the battery and output capacitor. The battery charger stage is a buck converter [23],[24].

For renewable energy systems, a DC-DC converter with energy storage battery is suggested in this thesis. Voltage Regulator Battery Energy Storage System is the name of this system. The suggested system connects a generator-turbine for wind energy to an unregulated rectifier. This system is immediately connected to a photovoltaic (PV) array in the case of solar energy[25]. Switch-mode DC/AC converter connects the Voltage Regulator Battery Energy Storage System(VR-BESS) to the ac utility source.

**2. BRUSHLESS DC MOTOR**

**2.1 General Voltage Regulator (V.R):**

A typical BLDC motor will have a permanent magnet rotor and three stainless steel stator windings. The strong resistance of magnets and stainless steel makes it possible to disregard rotor induced currents. Even though damper windings aren't taken into account, the circuit equation of the three stator windings in phase variables is derived and can be stated as,

$$\begin{bmatrix} v_r \\ v_y \\ v_b \end{bmatrix} = \begin{bmatrix} R_{sb} & 0 & 0 \\ 0 & R_{sb} & 0 \\ 0 & 0 & R_{sb} \end{bmatrix} \begin{bmatrix} i_r \\ i_y \\ i_b \end{bmatrix} + \frac{d}{dt} \begin{bmatrix} L_{rr} & L_{ry} & L_{rb} \\ L_{yr} & L_{yy} & L_{yb} \\ L_{br} & L_{by} & L_{bb} \end{bmatrix} \begin{bmatrix} i_r \\ i_y \\ i_b \end{bmatrix} + \begin{bmatrix} e_r \\ e_y \\ e_b \end{bmatrix} \tag{2.1}$$

where the stator phase voltage is written as  $v_r, v_y$  and  $v_b$ ,  $R_{sb}$  stator resistance of BLDC motor, stator phase current is written as  $i_r, i_y$  and  $i_b$ . And  $L_{rr}, L_{yy}, L_{bb}$  and  $L_{ry}, L_{yb}$  and  $L_{br}$  are the self-inductance and mutual inductance of stator winding respectively. The back electromagnetic force of each phase as  $e_r, e_y$  and  $e_b$ . The impedance of all the field winding was believed to be equal. It's also been suggested that if the rotor reluctance does not vary with angle since there isn't a prominent rotor, then the inductor L

$$L_{rr} = L_{yy} = L_{bb} = L_s \tag{2.2}$$

$$L_{ry} = L_{yr} = L_{rb} = L_{br} = L_{yb} = L_{by} = M \tag{2.3}$$

Substitute the value of (2.2) and (2.3) in Equation of (2.1)

$$\begin{bmatrix} v_r \\ v_y \\ v_b \end{bmatrix} = \begin{bmatrix} R_{sb} & 0 & 0 \\ 0 & R_{sb} & 0 \\ 0 & 0 & R_{sb} \end{bmatrix} \begin{bmatrix} i_r \\ i_y \\ i_b \end{bmatrix} + \frac{d}{dt} \begin{bmatrix} L & M & M \\ M & L & M \\ M & M & L \end{bmatrix} \begin{bmatrix} i_r \\ i_y \\ i_b \end{bmatrix} + \begin{bmatrix} e_r \\ e_y \\ e_b \end{bmatrix} \tag{2.4}$$

The  $v_r, v_y$  and  $v_b$  are the phase voltage of stator and designed as  $v_r=v_{r0}-v_{n0}$ ,  $v_y=v_{y0}-v_{n0}$  and  $v_b=v_{b0}-v_{n0}$ , where  $v_{r0}, v_{y0}, v_{b0}$  and  $v_{n0}$  are the voltages referring to the zero reference in three phase and neutral voltages potential at the dc-link's mid-point. The stator current is under balanced condition then the equation will be

$$i_r + i_y + i_b = 0 \tag{2.5}$$

As a result of this, the inductances matrix in the models is simplified as

$$Mi_r + Mi_y + Mi_b = 0 \tag{2.6}$$

$$Mi_y + Mi_b = -Mi_r \tag{2.7}$$

As a result, we can express the state space equation as

$$\begin{bmatrix} v_r \\ v_y \\ v_b \end{bmatrix} = \begin{bmatrix} R_{sb} & 0 & 0 \\ 0 & R_{sb} & 0 \\ 0 & 0 & R_{sb} \end{bmatrix} \begin{bmatrix} i_r \\ i_y \\ i_b \end{bmatrix} + \frac{d}{dt} \begin{bmatrix} L_s - M & 0 & 0 \\ 0 & L_s - M & 0 \\ 0 & 0 & L_s - M \end{bmatrix} \begin{bmatrix} i_r \\ i_y \\ i_b \end{bmatrix} + \begin{bmatrix} e_r \\ e_y \\ e_b \end{bmatrix} \tag{2.8}$$

It is assumed that the back EMFs  $e_r$ ,  $e_y$  and  $e_b$  have a trapezoidal wave from the source then the equation will be

$$\begin{bmatrix} e_r \\ e_y \\ e_b \end{bmatrix} = \omega_{mb} \varphi_{mb} \begin{bmatrix} f_r(\theta_{rb}) \\ f_y(\theta_{rb}) \\ f_b(\theta_{rb}) \end{bmatrix} \tag{2.9}$$

where  $\omega_{mb}$  is the rotor angular velocity of BLDC rotor in rad/sec,  $\varphi_{mb}$  is the flux-link of motor,  $\theta_{rb}$  is the rotational orientation of the rotor in radians,  $f_r(\theta_{rb})$ ,  $f_y(\theta_{rb})$  as well as  $f_b(\theta_{rb})$  are the function of trapezoidal waveform same as back emf phase voltage with the magnitude of  $\pm 1$  and it does not have sharp corners. The back emf is composed of the continuous functions of the flux linkages derivatives. The electromagnetic torque of BLDC motor is given by,

$$T_{eb} = [e_r i_r + e_y i_y + e_b i_b] / \omega_{mb} \tag{2.10}$$

It is significant to examine that, the phase voltage is identical to armature voltage of a brushed dc machine; hence it is referred to as a PM brushless drive system. The moment of inertia is given by

$$J \frac{d\omega_{mb}}{dt} + B\omega_{mb} = [T_{eb} - T_{Lb}] \tag{2.11}$$

BLDC motor load torque is denoted by  $T_{Lb}$ , where  $J$  is the inertia moment,  $B$  is the inertia co-efficient, and. An equation describing the relationship between rotor speed and location is as

$$\frac{d\theta_{rb}}{dt} = \frac{p_b}{2} \omega_{mb} \tag{2.12}$$

The inertia coefficient  $B$  is small value so it is easily ignored and the rotor position  $\theta_{rb}$  is represented in Equation (4.12) which repeats every  $2\pi$  radians. Neutral point potential in respect to ground voltage  $v_{no}$  must be resolved to prevent voltage unbalance and imitate motor function. By solving above equation and it is given as,

$$\begin{aligned} v_{ro} + v_{yo} + v_{bo} - 3v_{no} &= R_{sb}(i_r + i_y + i_b) + (L_s - M) (p_b i_r + \\ & p_b i_y + p_b i_b) + (e_r + e_y + e_b) \end{aligned} \tag{2.13}$$

Substitute the Equation (2.5) in above Equation (2.13), then equation will be

$$v_{ro} + v_{yo} + v_{bo} - 3v_{no} = (e_r + e_y + e_b) \tag{2.14}$$

$$v_{no} = [(v_{ro} + v_{yo} + v_{bo}) - (e_r + e_y + e_b)] / 3 \tag{2.15}$$

Finally, substitute all the relevant equation in the state space equation, will get

$$x = Ax + Bu + Ce \tag{2.16}$$

$$x = [i_r \ i_y \ i_b \ \omega_{mb} \ \theta_{rb}]^T \tag{2.17}$$

**3. SOLAR ENERGY SYSTEM**

**3.1 Design and modeling of solar power system:**

The PV converts solar energy into DC power by getting sunlight. A large number of solar cells are connected in series and parallel to make a solar array, which provides the required current and voltage. A battery, shunt resistance, series resistance, and diode can be used to form a PV cell. With the favor of MPPT enabled power electronic circuits, the solar photovoltaic (SPV) system supplies power to the load. Off-grid or stand-alone systems use solar energy which is directly given into the load, whereas ongrid or grid powered systems that is directly fed into the grid. The effectiveness of solar photovoltaic (SPV) arrays is greatly affected by variables in the surrounding environment. Both Ali Lamkaddem and Khalil Kassmi (2016). Figure 3.1 shows the comparable circuit of a solar cell.

Figure 3.1 depicts the current output of the aforementioned circuit when KCL is applied.

$$I_{pv} = I_{ph} - I_D - I_{Le} \tag{3.1}$$

where  $I_{ph}$  is the photon-generated current,  $I_D$  is the current in the diode, and  $I_{Le}$  is the leaking current in parallel resistance. And how much power does the solar panel put out?

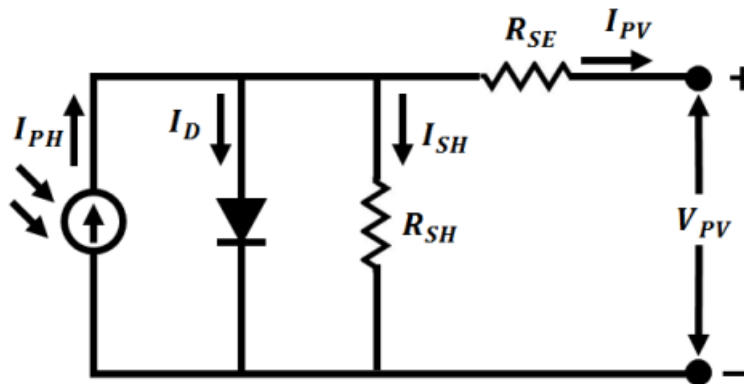


Fig 3.1: Equivalent circuit of Solar cell

$$I_D = I_s \left[ \exp \left( \frac{V + IR_{se}}{\alpha} \right) - 1 \right] \tag{3.2}$$

$$I_{Le} = \frac{V + IR_{se}}{R_{sh}} \tag{3.3}$$

Now substitute the value of  $I_D$  and  $I_{Le}$  in the Equation (3.1) and is obtained as

$$I_{pv} = I_{ph} - I_s \left[ \exp \left( \frac{V + IR_{se}}{\alpha} \right) - 1 \right] - \left( \frac{V + IR_{se}}{R_{sh}} \right) \tag{3.4}$$

where  $\alpha = B$ , is the thermal constant,  $n$  is the amount of cells in a sequence that are linked,  $B$  is the factor of ideality,  $k$  is atmospheric temperature-dependent thermal voltage and  $R_{se}$  is the series resistance. In both the loaded and unloaded states, the open circuit voltage and short circuit current are determined.

$$V_{oc} = \frac{AkT}{q} \ln \left( \frac{I_{Le}}{I} + 1 \right) \tag{3.5}$$

$$I_{sc} \approx I_{pv} \tag{3.6}$$

The amount of sunlight incident on the solar panel which directly influence the production of charge carriers and thereby current is generated in device. Since the resistance in a series connection is low and the resistance in a parallel connection is high, a parallel connection is used instead. Due to the dependence of solar panel output on both solar irradiance and temperature, the corresponding equation is

$$I_{pv} = (I_{pv,N} + K_T \Delta T) \frac{H}{H_n} \tag{3.7}$$

Saturation current of a diode is

$$I_s = I_{s,N} \left(\frac{T_{act}}{T_{ref}}\right)^3 \exp\left[\frac{qE_g}{AK} \left(\frac{1}{T_{act}} - \frac{1}{T_{ref}}\right)\right] \tag{3.8}$$

A parallel connection is preferred over a series one because of the large resistance in parallel. Due to the dependence of solar panel output on both solar irradiance and temperature, the corresponding equation is

$$I_{s,N} = \frac{I_{sc,N} + K_T \Delta T}{\exp\left(\frac{V_{oc,N} + K_T \Delta T}{\alpha V_T}\right) - 1} \tag{3.9}$$

There are three solar modules are utilized with the peak power capacity of 950W which are mounted in series for optimal performance. SPV arrays can be constructed with a wide variety of solar photovoltaic (SPV) cells, such as those made of mono-crystalline silicon, poly-crystalline silicon, or amorphous silicon (also known as thin film solar cells). Most solar panels today use mono crystalline cells since they have proven to be the most reliable.

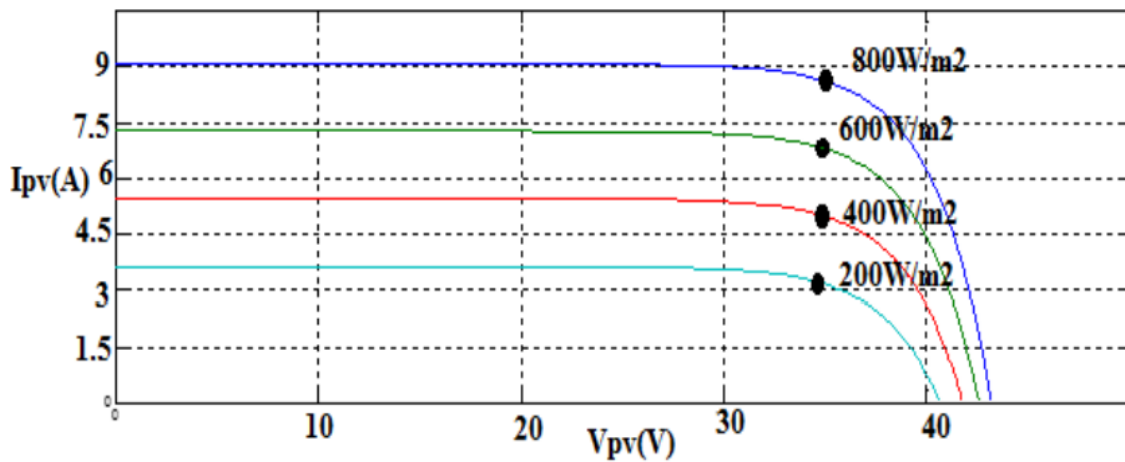


Figure 3.2 Changes in solar radiation I-V characteristics

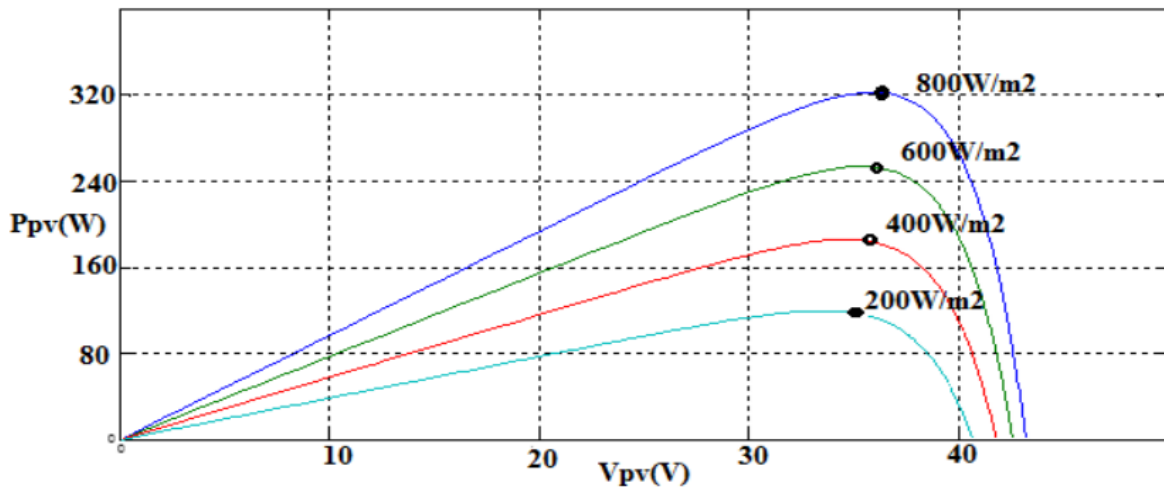


Figure 3.3 Changes in solar radiation P-V characteristics

**3.2 Maximum power point tracking techniques (MPPT):**

Variations in solar irradiance and temperature produce time-varying solar I-V and P-V characteristics, as seen in Figures 3.2 and 3.3. Maximum power point tracking is a method for determining peak power at any operating point by monitoring thermal performance and load resistance. To achieve this goal, a number of maximum power point tracking (MPPT) methods can be used. Perturbation and Observation (P&O), Incremental Conductance (Inc Cond), Fractional Open Circuit Voltage/Current, Hill Climbing, Fuzzy Logic Control, Neural Networks, and many others are all examples of MPPT algorithms (Zarko Zecevic & Maja Rolevski, 2020). Boualem Bendib et al. (2015) compare and contrast many MPPT control strategies. The number of sensors required, the price, the level of sophistication, the effective convergence speed range, the precision of monitoring during changes in irradiance or temperature, the hardware required for implementation, and their use are all variables.

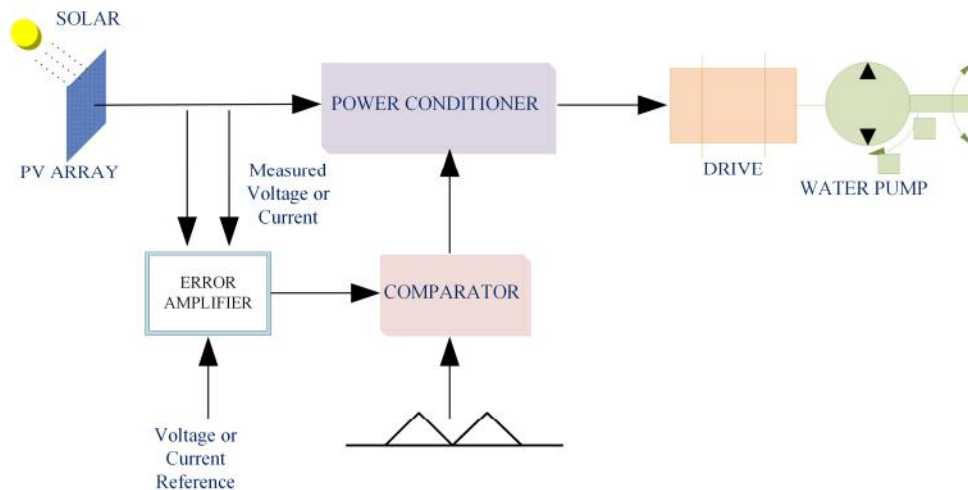


Figure 3.4 Generalized structure of MPPT controller for BLDC driven water-pumping system

Figure 3.4 shows the bare bones of an MPPT controller. The power conditioning unit consists of a DC-DC converter and a DC-AC inverter, and it receives electricity from the PV arrays.

To control the duty cycle, the PV array’s recorded voltage and current are compared to a reference signal, and the difference is amplified. The duty cycle of the converter switch is set by the error signal and maintained by pulses from the PWM signal to extract the maximum amount of power from the PV output voltage. The atmospheric temperature, tilt angle, irradiation, and temperature of the PV panels are major factor to ensure the power generation.

The temperature factor is depends on the site selection, latitude, climatic condition, environment and pollution which can be overcome by reducing the heating of the cells with the water cooling arrangement of the PV panels. The sun angle ( $\theta$ ) is angle between the suns light and ground, which should be within the range of  $(0-50^\circ)$  in cosine function, above this limit the generation become poor and the output almost negligible. The optimum tilt angle can improves the irradiation and amount of sun light incident on the panel with the mechanical controller to track the sun light intensity. The perfect relation of sun angle and output current (IPV) is given as

$$I_{PV} = I_{max} \text{Cos } \theta \tag{3.10}$$

When the solar panel is tilted at a shallow angle, it draws its maximum current ( $I_{max}$ ). The mechanical controller’s mechanism and other external elements are

The nonlinear V-I characteristics of solar panels make it impractical to extract maximum power throughout the entire generation, hence the PV array should operate at a given point, the location of which can be found by the following relation:

$$P = VI$$

$$\frac{dP}{dV} = I \frac{dV}{dV} + V \frac{dI}{dV} \tag{3.11}$$



At the greatest power point, where the derivative of the power is 0, the resultant equation is as

$$\frac{dP}{dV} = -\frac{I}{V} \quad (3.12)$$

Maximum power point operation is facilitated by knowing that dynamic impedance equals the negative slope of static impedance.

As long as the open circuit voltage ( $V_{oc}$ ) and output voltage of the solar panel remain constant, the controller will continue to raise the operating voltage until the derivative of power ( $Dp/Dv$ ) equals zero, at which point the output voltage will be referred to as peak operating voltage ( $V_{max}$ ). Maximum operating voltage is used to determine open circuit voltage, and this is achieved when the panel is exposed to uniform solar light without any load. The controller makes minor adjustments to the panel's operating voltage in order to maintain a consistent negative static and dynamic impedance. This allows for the maximum voltage of operation to be calculated, allowing for the maximum efficiency of PV panels to be attained. However, the P&O MPPT method and the incremental Conductance Method (IC) are two traditional tracking methods that are discussed in detail here.

### 3.2.1 Perturb and observe MPPT algorithm:

There is no need to keep track of any historical data with the P&O MPPT, and there are also no time-consuming or costly mathematical operations involved. The name "hill climbing algorithm" comes from the fact that this technique relies on a "perturbation and absorption loop" to achieve its goals. Detecting the voltage and current from the PV panel, calculating the power, and then adjusting the duty cycle of the DC-DC converter to achieve maximum power point all contribute to a fast-acting tracking system that significantly minimizes the amount of large-size capacitors.

It takes two sensors and some simple arithmetic to measure voltage and current. The technique starts with the converter's duty cycle and allows the user to fine-tune it by adding or subtracting from the error value. The PV voltage perturbation is increased in the direction of the maximum power point when the derivative ( $dP/dV > 0$ ) value is less than zero, and decreased in the opposite direction otherwise.

### 3.2.2 Incremental conductance MPPT algorithm:

The incremental conduction algorithm is superior than the P&O algorithm because of the rapid irradiation changes that occur in a changing atmosphere. Maximum power point and  $dP/dV$  polarity are determined at constant voltage. The duty cycle step size is set by the proportion of the PV array's instantaneous conductance to its incremental conductance.

## 4. METHODOLOGY

### 4.1 Configuration of proposed system:

The proposed water pumping system is shown in Fig. 4.1, along with a potential implementation of the system, in which a BLDC motor is used to operate a water pump. Through a boost converter and a voltage source inverter (VSI), a BLDC motor-pump gets its power from a PV array. The VSI is responsible for the electrical commutation of the BLDC motor, while the boost converter is the component that tracks the maximum power point of the PV array utilizing the InC algorithm. In order to perform an electronic commutation, an internal encoder produces three Hall-Effect signals. The VSI DC bus is powered by a single-phase power supply. A DC bus capacitor can be used for bidirectional power transfer thanks to a voltage source converter (VSC). When water pumping is not needed, the PV array can provide power to the grid. To facilitate power transfer between the grid and VSC while reducing harmonic current in the supply, an interface inductor is installed in the line. In order to control the supply voltage harmonics, an RC ripple filter is included.

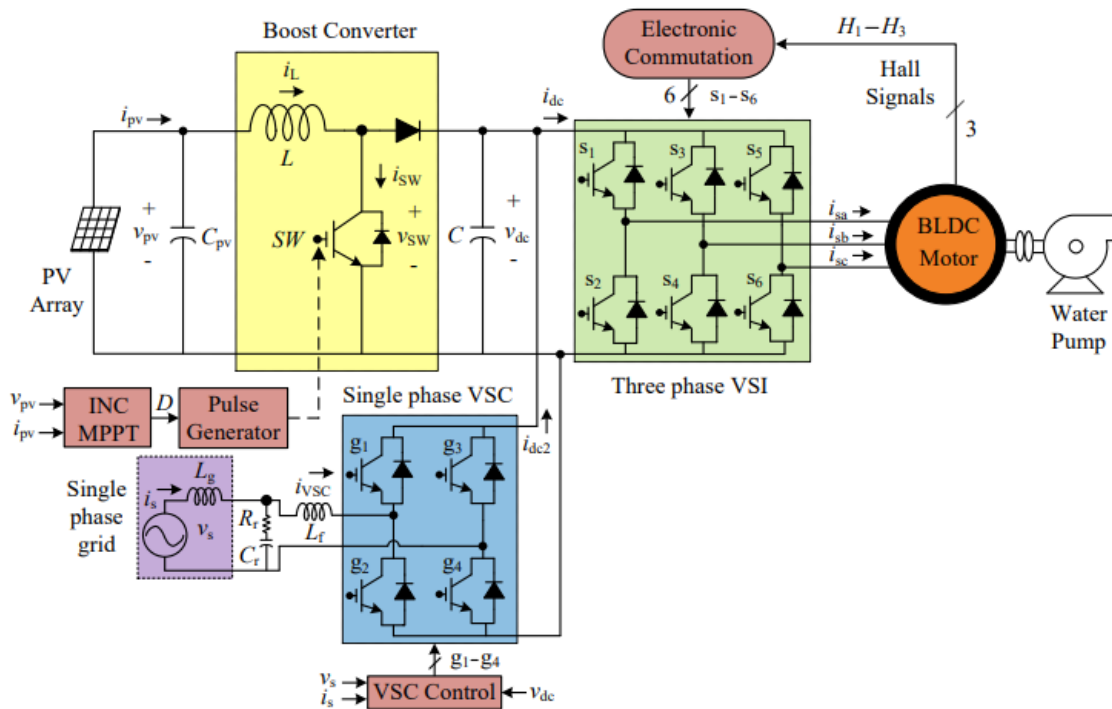


Fig.4.1 Schematic of the grid interactive PV array based water pumping system using a BLDC motor drive.

#### 4.2 Speed control of BLDC motor:

As was previously said, the phase current sensors are unnecessary with the proposed BLDC motor drive. It is preferred that the BLDC motor-pump be run at its rated speed regardless of environmental factors. The VSI DC bus voltage is maintained at the BLDC motor's rated DC voltage to accomplish this. By controlling the DC bus voltage and, in turn, the operating speed, a bidirectional power flow control ensures that the complete amount of power needed to run the water pumps is delivered. If there is no access to the grid or if the DC bus voltage drops below the rated DC voltage of the BLDC motor due to weather or other environmental factors, the speed will be controlled by the DC bus voltage.

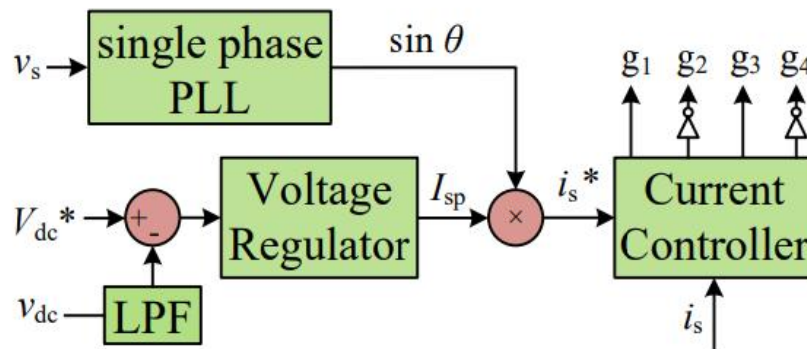


Fig. 4.2 UVT based bi-directional power flow control of VSC

#### 4.3 Bi-directional power flow control:

Grid-interactive PV generation allows for the construction of a trustworthy water pumping system and the optimal use of available resources. As can be seen in Fig. 2, a bi-directional power control is implemented using a UVT generation [20, 27-28] to enable power flow in both directions. This is the simplest method, and it's also the quickest and easiest to apply because it doesn't rely on a fancy mathematical model or algorithm. The utility grid voltage and current are synchronised using a Phase Locked Loop (PLL) with a single phase. At the fundamental frequency, it produces a supply voltage with a sinusoidal unit vector,  $\sin$ . On the other hand, by controlling the voltage on the DC bus,  $v_{dc}$ , we may extract



the amplitude of the supply current's basic component,  $I_{sp}$ . The voltage is controlled via a proportional-integral (PI) controller. A first-order low pass filter is applied to the detected  $v_{dc}$  signal in order to filter out the ripple noise. After being filtered,  $v_{dc}$  is compared to a constant,  $V_{dc}^*$ . Multiplying  $I_{sp}$  by  $\sin$  yields  $i_s^*$ , a crucial part of supply current. The gating pulses for VSC are generated by a current controller, which compares the detected supply current,  $i_s$ , to the nominal value,  $i_s^*$ , and processes the resulting error.

**4.4 Multilevel Inverter:**

These days, high power is needed by many industrial applications. Some industrial equipment, however, may function on only a medium or small amount of electricity. While some high-power motors could benefit from using a single, universal power supply, the other loads could be damaged. Utility and motor drive applications often call for medium voltage. Since its introduction in 1975, the multi-level inverter has served as an alternative in high-power and medium-voltage settings. An alternative to traditional inverters in high power and medium voltage industrial settings is the multilevel inverter.

Types of Multi-level inverters

- Diode clamped multilevel inverter
- Flying capacitors multilevel inverter
- Cascaded H- bridge multilevel inverter

**4.5 Three phase VSC and Multilevel inverter:**

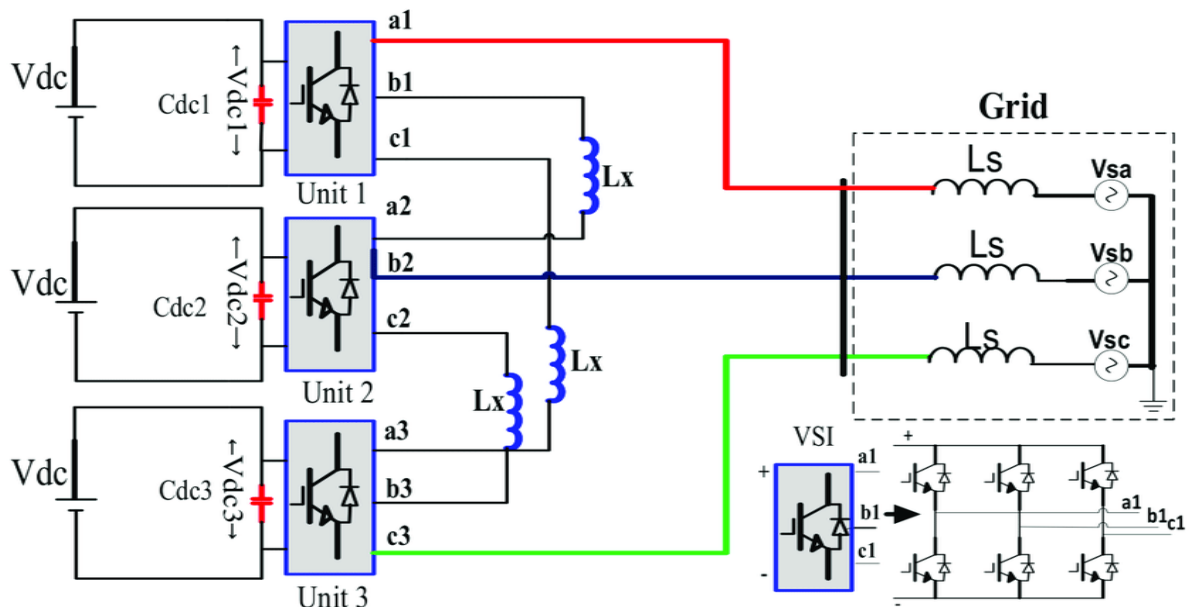


Fig 4.3: Three phase VSC and Multilevel inverter

A three-phase inverter working principle is, it includes three inverter switches with single-phase where each switch can be connected to load terminal. For the basic control system, the three switches operation can be synchronized so that single switch works at every 60 degrees of basic o/p waveform to create a line-to-line o/p waveform including six steps. This waveform includes a zero voltage stage among the two sections like positive & negative of the square-wave. Once PWM techniques based on the carrier are applied to these waveforms, then the basic shape of the waveform can be taken so that the third harmonic including its multiples will be canceled.

**5. MODELLING & SIMULATION**

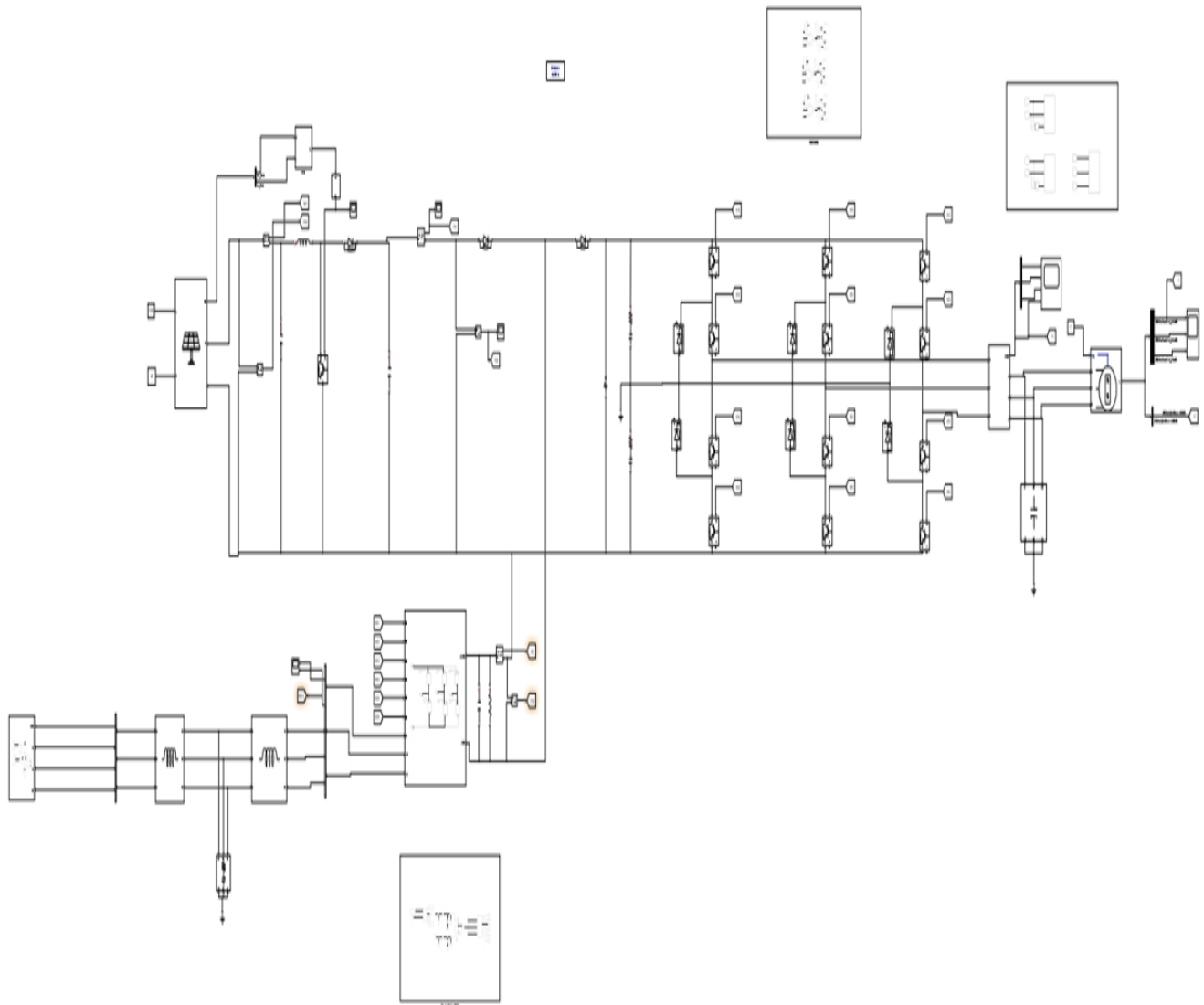


Figure 5.1: Simulation diagram of Grid based solar powered water pumping with 3 level multilevel inverter using BLDC motor drive

**Table 1: The Rated results**

**PV ARRAY**

Voltage(V)	Current(A)	Power(W)
235.2	54.52	12820

**Dc link capacitor**

Voltage(V)	Current(A)	Power(W)
238.5	12.29	3000

**Without Multilevel inverter**

Rotor speed(rad/sec)	Stator Current(A)	Three phase Voltage(V)
137.3	15.49	234.6

**With Multilevel inverter**

Rotor speed(rad/sec)	Stator Current(A)	Three phase Voltage(V)
155.9	31.07	300

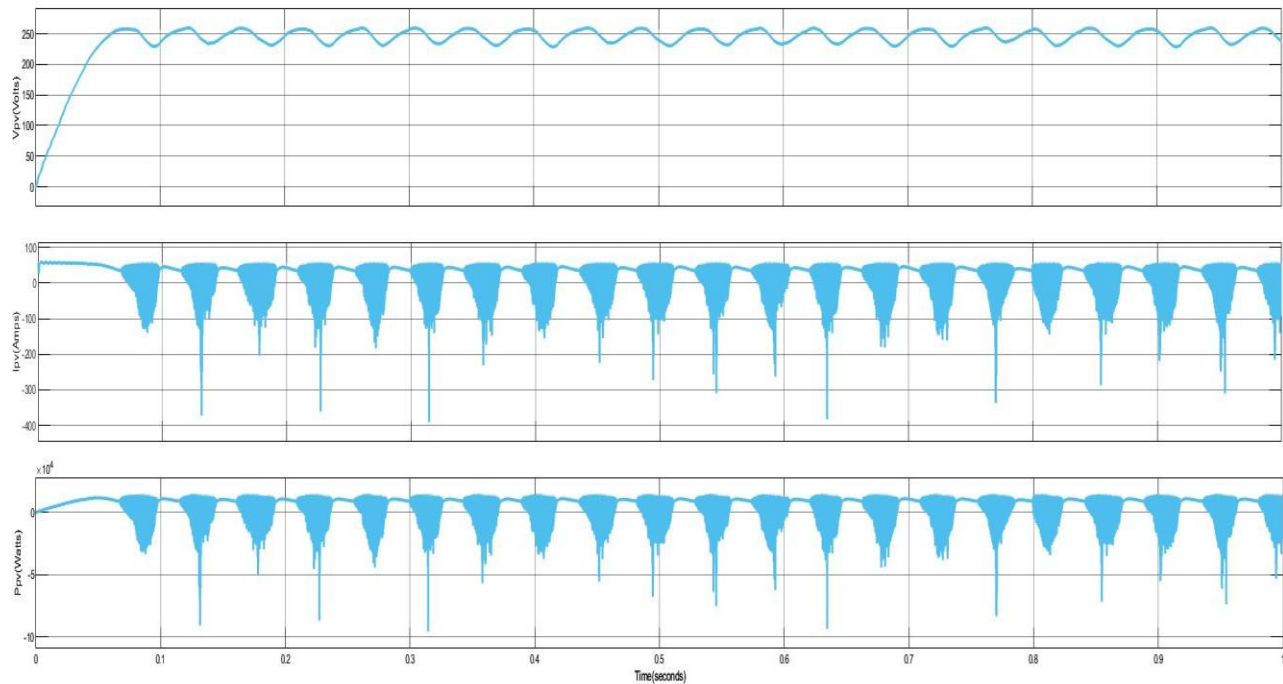


Fig 5.2: i) PV array Voltage  $V_{pv}$  ii) PV array current  $I_{pv}$  iii) PV array Power  $P_{pv}$

This fig 5.2 shows the results of the voltage which is coming from PV ( $V_{pv}$ ) and its current ( $I_{pv}$ ) and also shows how much power we are getting that is PV power is ( $P_{pv}$ ).

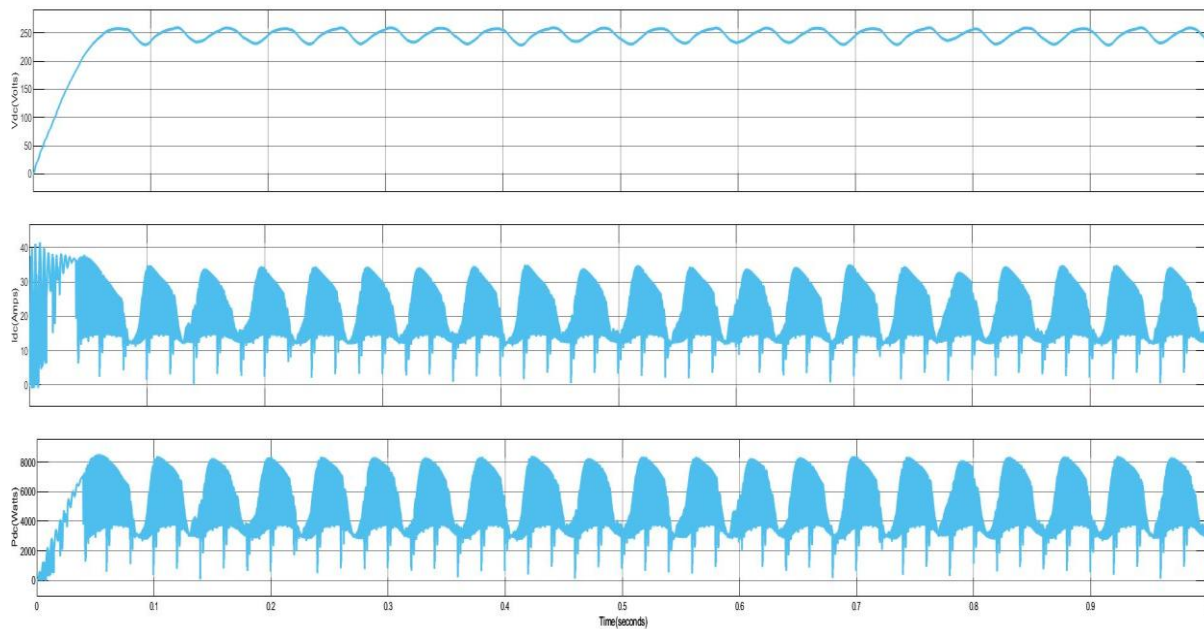


Fig 5.3: i) DC link capacitor voltage  $V_{dc}$  ii) DC link capacitor current  $I_{dc}$  iii) DC link capacitor power  $P_{dc}$

The figure 5.3 describes the graphs of DC link capacitor voltage and DC link capacitor current  $I_{dc}$  and also shown the power of DC link capacitor  $P_{dc}$ .

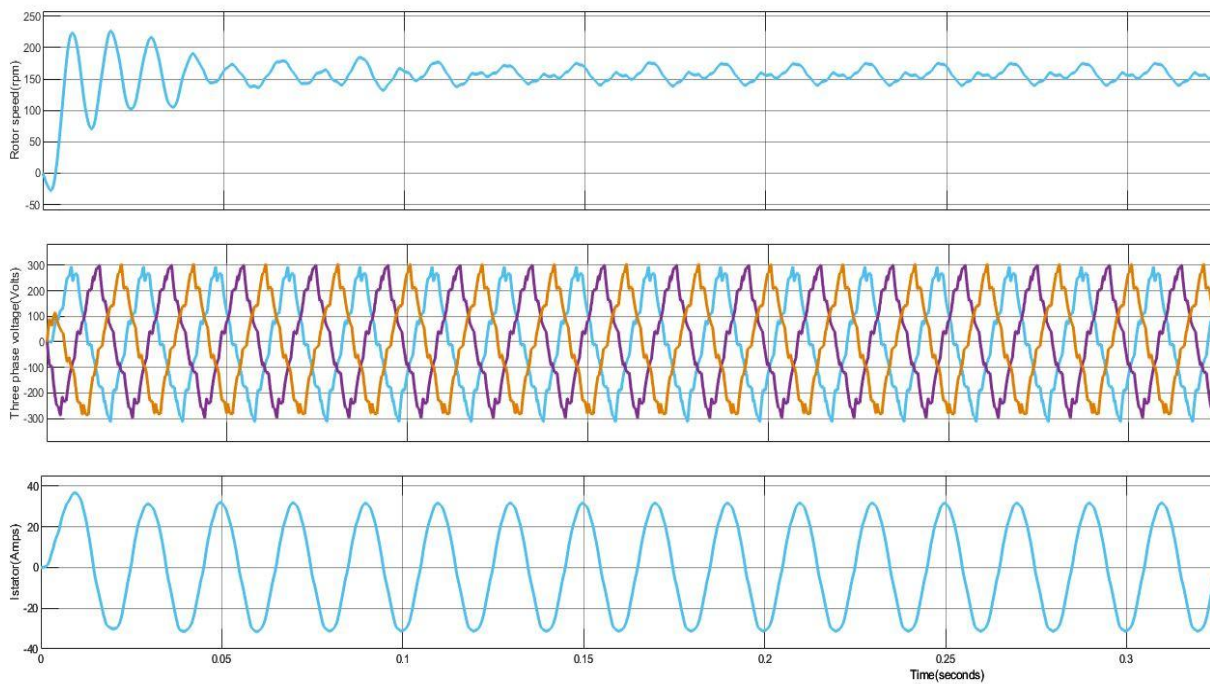


Fig 5.4: i) Rotor Speed ii) Three-phase Voltage iii) Stator Current

The figure 5.4 shows the simulation results for speed of rotor and three phase voltage and stator current.

## CONCLUSIONS

It has been proposed and proved that a PV array coupled with a BLDC motor drive can function as a grid-interactive single-phase water pumping system. VSC's ability to regulate electricity in both directions has allowed for optimal resource utilisation and water pumping at all times, regardless of the weather. The power distribution has been regulated with the use of a straightforward UVT generating method. The IEEE-519 standard for power quality has been fully implemented. Without the use of current sensing devices, BLDC motor-pump speed control has been obtained. To improve the entire system's efficiency, fundamental frequency VSI switching has been implemented. The proposed method has proven to be both a dependable water pumping system and a means of generating income through the sale of energy to the utility company during times when water pumping is unnecessary.

## REFERENCES

- [1] Abdouramani Dadjé, Noël Djongyang, Janvier Domra Kana & René Tchinda 2016, 'Maximum power point tracking methods for photovoltaic systems operating under partially shaded or rapidly variable insolation conditions: a review paper', *International Journal of Sustainable Engineering*, vol. 9, no. 4, pp. 224-239.
- [2] Alice Hepzibah, A & Premkumar, K 2020, 'ANFIS current-voltage controlled MPPT algorithm for solar powered brushless DC motor based water pump', *Electrical Engineering*, vol.102, pp. 421-435.
- [3] Sapavath Sreenu, Dr.Jalla Upendar, and Bogimi Sirisha "Analysis of Switched Impedance Source/Quasi-Impedance Source DC-DC Converters for Photovoltaic system", *International Journal of Applied Power Engineering(IJAPE)*, vol. 11, no.1, p-ISSN: 2252-8792, March-2022, doi:http://doi.org/10.11591/ijape.v11.i1.pp14-24.
- [4] Jalla Upendar, S.Ravi, Sapavath Sreenu and Bogimi Sirisha "Study and implementation of fuzzy based KY-boost converter for electric vehicle charging", *International Journal of Applied Power Engineering(IJAPE)*, vol. 11, no.1, p-ISSN: 2252-8792, March-2022, doi:http://doi.org/10.11591/ijape.v11.i1.pp98-108.
- [5] S.Sreenu, E.Ravinaik "Three Phase Multilevel Shunt Active Power Filters With Non Linear Loads for power quality Improvement" in *International Journal of Pure and Applied Mathematics(IJPAM)* (Scopus Indexed Journal), Volume 118 No. 24 2018, ISSN: 1314-3395 in Dr.B.V.Raju Institute of technology - Narsapur, Medak , Telangana, during 20th and 21st April 2018.
- [6] S.Sreenu, A.Miurali & A.L.Sahitya "A novel soft switching converter with high voltage gain and amplified efficiency for photovoltaic applications", in the second international conference on recent Innovations in engineering and Technology(ICRIEAT-2017) Organized by "Aurora"s scientific , technologies and research Academy, Hyderabad" Held on 21st&22nd December -2017

- [7] Bataineh, K 2018, 'Improved hybrid algorithms-based MPPT algorithm for PV system operating under severe weather conditions', *IET Power Electronics*, vol. 12, no. 4, pp.703-711.
- [8] Belhachat, F & Larbes, C 2017, 'Global maximum power point tracking based on ANFIS approach for PV array configurations under partial shading conditions', *Renewable and Sustainable Energy Reviews*, vol. 77, pp. 875-889.
- [9] Ajmeera Sampath Kumar, Balu Banavath and S.Sreenu "A Novel reduced capacitance with Quasi-Z-Source inverter for RES application", Published in *Pramana Research Journal*, Issue No:6, volume.9, 2019, pp: 1279-1291, ISSN:2249-2976.
- [10] Balu Banavath, Ajmeera Sampath Kumar and S.Sreenu, "Comparative Study of Various PWM methodologies for Grid connected Inverter for RES Application", Published in *Pramana Research Journal*, Issue No:6, volume.9, 2019, pp: 1279-1291, ISSN:2249-2976.
- [11] Da Luz, CMA, Vicente, EM & Tofoli, FL 2020, 'Experimental evaluation of global maximum power point techniques under partial shading conditions', *Solar Energy*, vol. 196, pp. 49-73.
- [12] Danandeh, MA 2018, 'A new architecture of INC-fuzzy hybrid method for tracking maximum power point in PV cells', *Solar Energy*, vol. 171, pp. 692-703.
- [13] Faiza Belhachat & Cherif Larbes 2017, 'Global maximum power point tracking based on ANFIS approach for PV array configurations under partial shading conditions', *Renewable and Sustainable Energy Reviews*, vol. 77, pp. 875-889.
- [14] Fernando Lessa Tofoli, Dênis de Castro Pereira & Wesley Josias de Paula 2015, 'Comparative Study of Maximum Power Point Tracking Techniques for Photovoltaic Systems', *International Journal of Photoenergy*, vol. 2015, Article ID 812582, pp. 1-10.
- [15] Gosumbonggot, Jirada & Goro Fujita 2019, 'Partial shading detection and global maximum power point tracking algorithm for photovoltaic with the variation of irradiation and temperature', *Energies*, vol.12, no. 202, pp. 1-22.
- [16] Houria Boumaaraf, Abdelaziz Talha & Omar Bouhali 2015, 'A threephase NPC grid-connected inverter for photovoltaic applications using neural network MPPT', *Renewable and Sustainable Energy Reviews*, vol. 49, pp. 1171-1179.
- [17] Hsu, TW, Wu, HH, Tsai, DL & Wei, CL 2018, 'Photovoltaic energy harvester with fractional open-circuit voltage based maximum power point tracking circuit', *IEEE Transactions on Circuits and Systems II: Express Briefs*, vol. 66, no. 2, pp. 257-261.
- [18] Hu, K, Cao, S, Li, W & Zhu, F 2019, 'An Improved Particle Swarm Optimization Algorithm Suitable for Photovoltaic Power Tracking under Partial Shading Conditions', *IEEE Access*, vol.7, pp.143217-143232.
- [19] Jirada Gosumbonggot 2016, 'Maximum Power Point Tracking Method using Perturb and Observe Algorithm for Small Scale DC Voltage Converter', *Procedia Computer Science*, vol. 86, pp. 421-424.
- [20] Kante Visweswara 2014, 'An Investigation of Incremental Conductance based Maximum Power Point Tracking for Photovoltaic System', *Energy Procedia*, vol. 54, pp.11-20.
- [21] Khanaki, Razieh, Mohd Radzi, Mohd Amran & Marhaban, Mohammad Hamiruce 2014, 'Artificial neural network based maximum power point tracking controller for photovoltaic standalone system', *International Journal of Green Energy*, vol.13, no.3, pp. 1543-5075.
- [22] Kumar, R, Khandelwal, S, Upadhyay, P & Pulipaka, S 2019, 'Global maximum power point tracking using variable sampling time and pv curve region shifting technique along with incremental conductance for partially shaded photovoltaic systems', *Solar Energy*, vol.189, pp.151-178.
- [23] Li, G, Jin, Y, Akram, MW, Chen, X & Ji, J 2018, 'Application of bio-inspired algorithms in maximum power point tracking for PV systems under partial shading conditions—A review', *Renewable and Sustainable Energy Reviews*, vol. 81, pp.840-873.
- [24] Li, W, Zhang, G, Pan, T, Zhang, Z, Geng, Y & Wang, J 2019, A Lipschitz Optimization-Based MPPT Algorithm for Photovoltaic System Under Partial Shading Condition. *IEEE Access*, vol.7, pp.126323-126333.
- [25] Lyden, S & Haque, ME 2015, 'Maximum Power Point Tracking techniques for photovoltaic systems: A comprehensive review and comparative analysis', *Renewable and Sustainable Energy Reviews*, vol. 52, pp. 1504-1518.